

## Hyperbranched Conjugated Polyelectrolyte Bilayers for Solar-Cell Applications

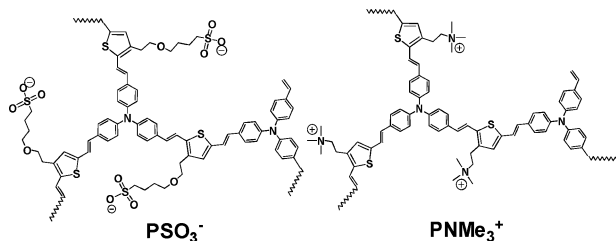
Prasad Taranekar, Qiquan Qiao, Hui Jiang, Ion Ghiviriga, Kirk S. Schanze,\* and John R. Reynolds\*

Department of Chemistry, Center for Macromolecular Science and Engineering, University of Florida,  
P.O. Box 117200, Gainesville, Florida 32611-7200

Received May 7, 2007; E-mail: reynolds@chem.ufl.edu; kschanze@chem.ufl.edu

Conjugated polyelectrolytes (CPEs) have been proposed as energy and charge transporting materials for a number of potential applications which include polymer light emitting diodes<sup>1</sup> and polymer photovoltaic cells.<sup>2</sup> With their polyelectrolyte nature, CPEs can be self-assembled by alternating adsorption of anionic and cationic polyelectrolytes, or related dendritic macromolecules, at interfaces.<sup>3,4</sup> While dendrimers have been of wide interest because of their highly controllable structures, hyperbranched polymers (HBPs) provide an excellent alternative with the added advantage of being easily synthesized in one reaction while showing comparable properties.<sup>5</sup> Compared to linear conjugated polymers, the incorporation of hyperbranched structure is advantageous because of low viscosity, high solubility, tunable emission color,<sup>6</sup> and disrupted inter- and intramolecular charge-transfer properties.<sup>7</sup>

Here, we report a new family of materials which combine the properties of both CPEs and HBPs. This work demonstrates a first example of the synthesis of hyperbranched conjugated polyelectrolytes (HB-CPEs), their self-assembly and application involving ionic hyperbranched conjugated polymer sensitized TiO<sub>2</sub> solar cells. The self-assembly driven by ionic interactions of oppositely charged HB-CPEs results in an increased chromophore concentration. This allows enhanced optical density and efficient light harvesting and possibly facilitates an enhanced energy and charge migration in the hybrid cell. The structures of both anionic (PSO<sub>3</sub><sup>−</sup>) and cationic (PNMe<sub>3</sub><sup>+</sup>) HB-CPEs are shown in the graphic.



The synthesis of these hyperbranched polymers was performed using the A<sub>3</sub> + B<sub>2</sub> type approach based on Heck polycondensation.<sup>8</sup> The monomer and polymer syntheses are detailed in the Supporting Information (SI). The polymers are readily soluble in polar organic solvents including MeOH, DMF, and DMSO and are partially soluble in water and insoluble in acetone, THF, and chloroform. The purpose of conjugating thiophene and triphenylamine vinylene groups is to allow spectral broadening for enhanced visible light absorption, thereby potentially increasing the amount of charge injected into the TiO<sub>2</sub>. In addition to the electronic band gap, the HB-CPEs can be self-assembled into bilayer structures to further enhance the optical density allowing efficient excited-state charge transfer to the TiO<sub>2</sub> acceptor while ensuring that the photo-oxidized polymer is easily reduced by the electrolyte.

The HB-CPEs were characterized using NMR, FTIR, and viscometry techniques (SI). Pulsed gradient spin echo (PSGE) NMR

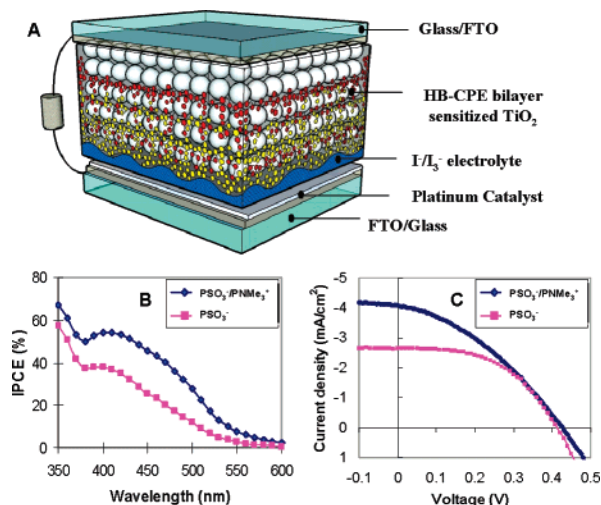
was used to estimate the HB-CPE molecular weights which yielded  $M = 3500$  Da for the PNMe<sub>3</sub><sup>+</sup> and  $M = 3200$  Da for PSO<sub>3</sub><sup>−</sup> (details in SI), and these low values may account for their propensity to penetrate into the TiO<sub>2</sub>. The molecular weights are within the range as reported earlier for non-ionic HB polymers synthesized via Heck coupling.<sup>8b</sup> It should be noted that this method does not provide any information on polydispersity, and GPC was not carried out owing to solvent incompatibility. The intrinsic viscosity [ $\eta$ ] was determined to be 0.15 and 0.11 for PSO<sub>3</sub><sup>−</sup> and PNMe<sub>3</sub><sup>+</sup>, respectively (SI Figure S3). It was found that even with the addition of salt the HB-CPEs expand their hydrodynamic volumes, resulting in the observed viscosity increase indicating a positive polyelectrolyte effect.<sup>9</sup>

The photophysical results, summarized in Table 1, show both PSO<sub>3</sub><sup>−</sup> and PNMe<sub>3</sub><sup>+</sup> to be fluorescent (SI Figure S4A) and have similar photophysical properties. The normalized absorption and fluorescence spectra of PSO<sub>3</sub><sup>−</sup> and PNMe<sub>3</sub><sup>+</sup> in methanol and water are shown in SI Figure S4B. This pair of solvents was selected on the basis of our previous work on linear conjugated polyelectrolytes, which indicates that MeOH is a “good solvent” (i.e., the polymers exist in an isolated state with minimal aggregation) and H<sub>2</sub>O is a “poor solvent” (i.e., the polymers exist as aggregates).<sup>2a,10</sup> Compared to MeOH, aqueous solutions of the polymers exhibit a broader absorption spectrum with a blue-shifted band max, decreased molar extinction coefficient, and a red-shifted fluorescence spectrum with a much decreased quantum yield. The time-resolved fluorescence was measured at wavelengths corresponding closely to the fluorescence maximum, and the decay curves were sufficiently fitted with two exponential terms. In all cases, the decays are characterized by a large amplitude, short-lifetime component (~90%, ~1.4 ns), and a low-amplitude component (~10%) with a lifetime of >10 ns. On the basis of these photophysical properties, it is reasonable to speculate that both polymers are expanded (well solvated) in a good solvent such as methanol and collapsed (poorly solvated) in a poor solvent such as water.

The ground-state oxidation potentials of the PNMe<sub>3</sub><sup>+</sup> and PSO<sub>3</sub><sup>−</sup> are 0.5 and 0.4 V versus saturated calomel electrode (SCE), respectively [estimated by differential pulse voltammetry (DPV) in conjunction with cyclic voltammetry (CV)], compared to that of the oxidation potential (0.1 V versus SCE) of the redox pair I<sup>−</sup>/I<sub>3</sub><sup>−</sup>.<sup>11</sup> The excited-state oxidation potentials are −1.7 and −1.8 V versus SCE, as calculated by  $E(P^*/P^+) = E(P/P^+) - E(P^*)$ , where  $E(P/P^+)$  is the potential of the polymers and  $E(P^*)$  is the energy of the relaxed singlet state as estimated from the fluorescence  $\lambda_{\text{max}}$  values of HB-CPE films. The excited-state oxidation potentials of PNMe<sub>3</sub><sup>+</sup> and PSO<sub>3</sub><sup>−</sup> are sufficiently negative of the TiO<sub>2</sub> conduction band (−0.42 V versus SCE), such that charge injection into the semiconductor is anticipated to be efficient.<sup>12</sup> This indicates that there is an energetic driving force for the electron and hole

**Table 1.** Photophysical Studies of the HB-CPEs in MeOH and Water

HB-CPEs	$\lambda_{\text{max}}$ [nm] absorption ( $\epsilon$ ) $\text{M}^{-1} \text{cm}^{-1}$	$\lambda_{\text{max}}$ emission nm	quantum yield % $\phi$	lifetime ( $\tau$ ) ns
$\text{PNMe}_3^+$ in MeOH	447, ( $2.4 \times 10^4$ )	555	6.0	1.3 (91%); 15.8 (9%)
$\text{PNMe}_3^+$ in $\text{H}_2\text{O}$	425, ( $1.9 \times 10^4$ )	590	0.5	1.5 (89%); 13.9 (11%)
$\text{PSO}_3^-$ in MeOH	405, ( $2.1 \times 10^4$ )	540	8	1.4 (92%); 15.7 (8%)
$\text{PSO}_3^-$ in $\text{H}_2\text{O}$	403, ( $1.5 \times 10^4$ )	570	0.4	1.2 (89%); 11.0 (11%)

**Figure 1.** (A) HB-CPE bilayer  $\text{TiO}_2$  solar cell configuration; (B–C) HB-CPE sensitized  $\text{TiO}_2$  cells comparing monolayer and self-assembled bilayer HB-CPEs showing (B) IPCE spectral responses and (C)  $J$ - $V$  studies under AM 1.5 conditions.

separation within a  $\text{TiO}_2$ /HB-CPE regenerative photochemical cell in which the HB-CPE operates as the light absorbing material.

Nanostructured  $\text{TiO}_2$  solar cells with adsorbed layers of HB-CPEs were fabricated as monolayers and self-assembled bilayers with the latter shown schematically (details in SI) in Figure 1A. For clarity we have only shown the comparison of incident photon to electron conversion efficiencies (IPCE) and current density-voltage ( $J$ - $V$ ) characteristics of monolayer  $\text{PSO}_3^-$  and self-assembled  $\text{PSO}_3^-/\text{PNMe}_3^+$  bilayer sensitized  $\text{TiO}_2$  cells in Figure 1B/C. It is immediately evident that the bilayer cell yields a higher IPCE and  $J_{\text{sc}}$  than the monolayer cell.

This is confirmed in SI Figure S5 for IPCE and  $J$ - $V$  for monolayer  $\text{PNMe}_3^+$  and self-assembled bilayer  $\text{PNMe}_3^+/\text{PSO}_3^-$ , where  $\text{PNMe}_3^+$  is the first layer monolayer deposited on the  $\text{TiO}_2$ . Table 2 details a comparative analysis of both monolayers and bilayers.

The cells with only a monolayer of either HB-CPE have nearly identical IPCE values, however  $\text{PSO}_3^-$  results in a higher  $\eta$  due to an enhanced FF and  $J_{\text{sc}}$  when compared to  $\text{PNMe}_3^+$ . This is likely due to the sulfonate groups which can coordinate to  $\text{TiO}_2$  in a similar manner to  $-\text{COOH}$  groups<sup>13</sup> promoting forward interfacial electron transfer and reducing the number of trap sites.<sup>11b</sup> The same argument can be made when forming the bilayer  $\text{PSO}_3^-/\text{PNMe}_3^+$  cell, where  $\text{PSO}_3^-$  is the first layer as compared to the bilayer of  $\text{PNMe}_3^+/\text{PSO}_3^-$ . Nevertheless, both bilayers show a superior response in

**Table 2.** Photovoltaic Studies of the HB-CPE Sensitized  $\text{TiO}_2$  Cells<sup>a</sup>

structure	$V_{\text{oc}}$ V	$J_{\text{sc}}$ $\text{mA}/\text{cm}^2$	FF	$\eta$ (%)	IPCE
$\text{PSO}_3^-$	0.42	2.7	0.51	0.57	37%
$\text{PSO}_3^-/\text{PNMe}_3^+$	0.42	4.1	0.36	0.62	55%
$\text{PNMe}_3^+$	0.43	2.1	0.35	0.33	38%
$\text{PNMe}_3^+/\text{PSO}_3^-$	0.48	3.2	0.36	0.55	44%

<sup>a</sup> IPCE @400 nm.

IPCE and overall efficiency compared to their respective monolayers owing to increased chromophore density causing more light absorption in the bilayer as compared to either monolayer.

In conclusion, this study has led to the development of novel anionic and cationically charged HB-CPEs which could be utilized as polymer dyes coordinated to  $\text{TiO}_2$  and self-assembled into bilayers for solar-cell applications. The details of hybrid film structure using electron microscopy and atomic force microscopy will be reported in the future. Although the performance in terms of efficiency is lower compared to conventional cells, prospects are high for rapid improvement. Thus, these polymers and their self-assembly hold a viable promise for enhanced adhesion and energy harvesting properties for future hybrid solar cells and further investigation is underway.

**Acknowledgment.** The financial support for this work was provided by the DOE/BES (Grant DE-FG02-03ER15484).

**Supporting Information Available:** Experimental, synthesis, and characterization details of monomers and HB-CPEs polymers. This material is available free of charge via the Internet at <http://pubs.acs.org>.

## References

- (1) Kraft, A.; Grimsdale, A. C.; Holmes, A. B. *Angew. Chem., Int. Ed. Engl.* **1998**, *37*, 402–428. (b) Yang, R.; Wu, H.; Cao, Y.; Bazan, G. C. *J. Am. Chem. Soc.* **2006**, *128* (45), 14422–14423.
- (2) (a) Mwaura, J. K.; Zhao, X.; Jiang, H.; Schanze, K. S.; Reynolds, J. R. *Chem. Mater.* **2006**, *18* (26), 6109–6111. (b) Coakley, K. M.; McGehee, M. D. *Chem. Mater.* **2004**, *16*, 4533–4542. (c) Yang, X.; Loos, J. *Macromolecules* **2007**, *40* (5), 1353–1362.
- (3) (a) Decher, G.; Lvov, Y.; Schitt, J. *Thin Solid Films* **1994**, *244*, 772–777. (b) Clark, A. P.-Z.; Cadby, A. J.; Shen, C. K.-F.; Rubin, Y.; Tolbert, H. J. *Phys. Chem. B* **2006**, *110* (44), 22088–22096.
- (4) (a) Tsukruk, V. V.; Rinderspacher, F.; Bliznyuk, V. N. *Langmuir* **1997**, *13* (8), 2171–2176. (b) Tomalia, D. A.; Frechet, J. M. *Prog. Polym. Sci.* **2005**, *30*, 217–219.
- (5) (a) Fomine, S.; Fomina, L.; Guadarrama, P. *Macromol. Symp.* **2006**, *192* (1), 43–62. (b) Voit, B. J. *Polym. Sci., Part A: Polym. Chem.* **2005**, *43*, 2679–2699.
- (6) (a) Tomalia, D. A.; Naylor, A. M.; Goddard, W. A. *Angew. Chem.* **1990**, *29*, 138–175. (b) Voit, B. I. *Acta Polym.* **1995**, *46*, 87. (c) Sun, M.; Bo, Z. J. *Polym. Sci., Part A: Polym. Chem.* **2007**, *45* (1), 111–124.
- (7) (a) Yang, J. L.; He, Q. G.; Lin, H. Z.; Fan, J. J.; Bai, F. L. *Macromol. Rapid Commun.* **2001**, *22*, 1152–1157. (b) Ramakrishna, G.; Ghosh, H. N. *J. Phys. Chem. A* **2002**, *106* (11), 2545–2553.
- (8) (a) Choi, J.-Y.; Tan, L.-S.; Baek, J.-B. *Macromolecules* **2006**, *39* (26), 9057–9063. (b) Tanaka, S.; Iso, T.; Sugiyama, J.-I.; Takeuchi, K.; Ueda, M. *Synth. Met.* **2005**, *154*, 125–128.
- (9) (a) Choi, J.-Y.; Tan, L.-S.; Baek, J.-B. *Macromolecules* **2006**, *39* (26), 9057–9063. (b) Baek, J.-B.; Tan, L. S. *Macromolecules* **2006**, *39* (8), 2794–2803.
- (10) Jiang, H.; Zhao, X.; Schanze, K. S. *Langmuir* **2006**, *22*, 5541–5543.
- (11) (a) Lenzmann, F.; Krueger, J.; Burnside, S.; Brooks, K.; Gratzel, M.; Gal, D.; Rühle, S.; Cahen, D. J. *Phys. Chem. B* **2001**, *105*, 6347–6352. (b) Ramakrishna, G.; Ghosh, H. N. *Langmuir* **2003**, *19* (3), 505–508.
- (12) (a) Palomares, E.; Clifford, J. N.; Haque, S. A.; Lutz, T.; Durrant, J. R. *J. Am. Chem. Soc.* **2003**, *125* (2), 475–482. (b) Staniszewski, A.; Morris, A. J.; Ito, T.; Meyer, G. J. *J. Phys. Chem. B* **2007**, *111*, 6822–6828.
- (13) Krebs, F. C.; Spanggaard, H. *Chem. Mater.* **2005**, *17* (21), 5235–5237.

JA073216A